

Fig. 3. Dependence of the log(ionic conductivity) (□), log(real shear modulus) (○), and heat flow (solid line) on reciprocal temperature for the 10:1 AO:Li 0G6 complex.

be detected. Furthermore, the mechanical properties of the complex are solid-like at temperatures below the observable glass transition, which would not be the case for a phase separated material containing rubbery microdomains.

Instead, we advance an explanation for the extraordinary properties of this liquid crystal complex by invoking a high degree of coupling between mesogenic side groups and the ethylene oxide backbone which thereby inhibits the formation of helical conformations favored by “free” poly(ethylene oxide) chains. Within such helical arrangements the lithium ions would be tightly coordinated below T_g and effectively trapped. By suppressing the formation of such helical structures, an open ethylene oxide structure is obtained within which lithium ions are free to move and where empty sites exist for the ions to occupy. It is remarkable that a similar (but weaker) effect is observed in the amorphous material. It seems that insertion of rigid isophthalate units also inhibits helical formation, sufficient to provide a measure of ionic decoupling, but for the liquid crystal complex the open structure is further stabilized via the interactions between the liquid crystal side groups. It is worth noting that this view is supported by the continuity of behavior from the melt into the glassy state in both the heat capacity and electrical conductivity, indicating that the structure of the melt is not strongly influenced by temperature. In addition, the dissolution of the ions in the backbone does not swell the smectic layer and thus, the open network must be relatively unchanged at least in the direction normal to the smectic layers. This suggests that by careful engineering of the types of liquid crystal phase present, it should be possible to tailor the conductivity mechanism to particular applications.

It is also remarkable that the conductivity in the MeOC6G6 complex increases strongly (by several orders of magnitude) as the AO:Li ratio is decreased from 10:1 to

3:1. We should now be able to employ more concentrated polymer electrolytes than is presently possible with conventional materials. Transport number data for these electrolytes are not yet available, but it is tempting to speculate that the elimination of “cation trapping” within the ethylene oxide helix will lead to substantial increases in cation mobility. For many years this has been one of the principal goals of polymer electrolyte research.

Received: December 8, 1998
Final version: February 22, 1999

- [1] S. Druger, M. A. Ratner, A. Nitzan, *Solid State Ionics* **1986**, 18–19, 106.
- [2] C. A. Angell, *Solid State Ionics* **1986**, 18–19, 72.
- [3] R. J. Grant, M. D. Ingram, L. D. S. Turner, C. A. Vincent, *J. Phys. Chem.* **1978**, 82, 2838.
- [4] M. D. Ingram, *Curr. Opin. Solid State Mater. Sci.* **1997**, 2, 399.
- [5] C. A. Angell, C. Liu, E. Sanchez, *Nature* **1993**, 362, 137.
- [6] C. A. Angell, K. Xu, S.-S. Zhang, M. Videa, *Solid State Ionics* **1996**, 86–88, 17.
- [7] M. B. Armand, *Solid State Ionics* **1994**, 69, 309.
- [8] W. H. Meyer, *Adv. Mater.* **1998**, 10, 439.
- [9] C. A. Angell, C. T. Imrie, M. D. Ingram, *Polym. Int.* **1998**, 47, 9.
- [10] G. G. Cameron, J. L. Harvie, M. D. Ingram, *J. Chem. Soc. Faraday Discuss.* **1989**, 88, 55.
- [11] P. G. Bruce, C. A. Vincent, *J. Chem. Soc. Faraday Discuss.* **1989**, 88, 43.
- [12] T. Yamamoto, M. Inami, T. Kanabara, *Chem. Mater.* **1994**, 6, 44.
- [13] H. A. Every, F. Zhou, M. Forsyth, D. R. MacFarlane, *Electrochim. Acta* **1998**, 43, 1465.
- [14] F. B. Dias, S. V. Batty, G. Ungar, J. P. Voss, P. V. Wright, *J. Chem. Soc. Faraday Trans.* **1996**, 92, 2599.
- [15] F. B. Dias, S. V. Batty, A. Gupta, G. Ungar, J. P. Voss, P. V. Wright, *Electrochim. Acta* **1998**, 43, 1217.
- [16] G. S. McHattie, C. T. Imrie, M. D. Ingram, *Electrochim. Acta* **1998**, 43, 1151.
- [17] C. A. Angell, *Chem. Rev.* **1990**, 90, 523.
- [18] F. S. Howell, R. A. Bose, P. B. Macedo, C. T. Moynihan, *J. Phys. Chem.* **1974**, 78, 639.

Dissolution of Single-Walled Carbon Nanotubes**

By Mark A. Hamon, Jian Chen, Hui Hu, Yongsheng Chen, Misha E. Itkis, Apparao M. Rao, Peter C. Eklund, and Robert C. Haddon*

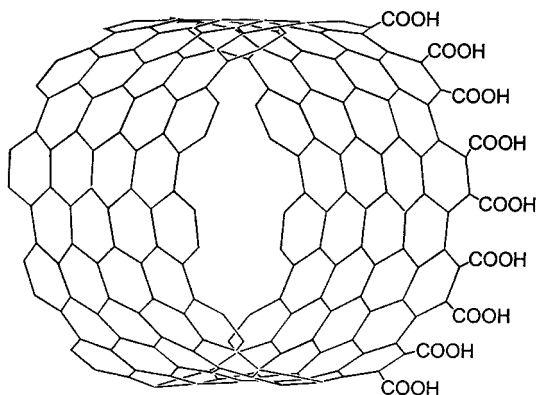
The scientific and technological potential of single-walled carbon nanotubes (SWNTs) has attracted considerable attention to this field. Previous studies have been carried out on solid, intractable forms of SWNTs.^[1–6] We have recently shown that end-group functionalization of short (100–300 nm in length)^[5] SWNTs allows the preparation of stable organic solutions of these materials.^[7] The prep-

[*] Prof. R. C. Haddon, M. A. Hamon, Dr. J. Chen, H. Hu, Dr. Y. Chen, Dr. M. E. Itkis, Dr. A. M. Rao, Dr. P. C. Eklund
Departments of Chemistry and Physics, Center for Applied Energy Research and Advanced Carbon Materials Center
University of Kentucky
Lexington, KY 40506-0055 (USA)

[**] We thank M. Thompson (Digital Instruments), for AFM measurements. This work was supported under the NSF Division of Materials Research MRSEC program; grant number DMR-9809686.

aration of these solutions has allowed the study of the chemistry of naked carbon nanotube metals and semiconductors, and the response of the band electronic structure of these materials to chemical modification. In the present manuscript we report additional details of the solubility properties of SWNTs and the factors that control the dissolution of these materials. As noted previously, these objects are to be considered as fullerene pipes,^[5] and with an atomic diameter of about 14 Å, there is a great deal of space inside the tubes (van der Waals internal diameter of about 10 Å), which is presumably occupied by solvent molecules when these cylindrical fullerenes dissolve.

Both the purification process and the shortening process terminate the open ends of the SWNTs with carboxylic acid groups.^[5,7] This is illustrated in Scheme 1 with the (10,10)-SWNT-COOH. The carboxylic acid groups can be converted into acylchloride groups by treatment with thionylchloride.^[5,7] The acid chloride-functionalized SWNTs are then susceptible to reaction with amines to give amides. If the latter reaction is carried out at elevated temperatures for 4 days, most of the SWNT bundles exfoliate to give individual SWNT macromolecules (Fig. 1) and small bundles that are soluble in organic solvents (s-SWNT).^[7] With lengths up to about 300 nm, these fullerene pipes contain ~50 000 carbon atoms in ~25 000 benzenoid rings, and have a molecular weight of ~600 000 D, which is approaching the high polymer regime. In the original report,^[7] we made use of the long-chain aliphatic amine octadecylamine [$\text{CH}_3(\text{CH}_2)_{17}\text{NH}_2$] to bring about the desired solubility properties of the functionalized SWNTs. In this work, we extend our studies to amide formation (Scheme 2A) from the alkyl-aryl amine 4-dodecyl-aniline [$4\text{-CH}_3(\text{CH}_2)_{13}\text{C}_6\text{H}_4\text{NH}_2$]. While the SWNT-derivative (Scheme 2B) is represented as an amide for convenience, it appears that the products exist primarily as imides (illustrated for (10,10)-SWNT).



Scheme 1. Structure of (10,10)-SWNT-COOH.

Most of the conventional analytical tools of organic chemistry can be used in the characterization of the s-SWNT.^[7,8] The IR spectrum (KBr pressed pellet), of the s-SWNT-CONH-4-C₆H₄(CH₂)₁₃CH₃ (Fig. 2 and Table 1) shows peaks at 2922 cm⁻¹ and 2843 cm⁻¹, which are due to

the C-H stretch modes in the alkyl chain (appearing at 2927 and 2849 cm⁻¹ in the parent amine). The amide carbonyl group appears as a broad peak at 1655 cm⁻¹. The sharp peak at 1519 cm⁻¹ is from the aromatic carbon-carbon bond stretch mode (1519 cm⁻¹ in the parent amine). The broad peak at 1598 cm⁻¹ is probably due to the N-H bend of the amide (1629 cm⁻¹ in the parent amine). The peak at 1450 cm⁻¹ is due to the C-H bend (1466 cm⁻¹ in the parent amine). Many of the same vibrational modes are seen in other forms of the SWNTs.^[7]

Table 1. Mid-IR spectra (KBr) of open SWNTs (SWNT-COR).

Group (R)	$\nu(\text{C-H})$ [cm ⁻¹]	$\nu(\text{C=O})$ [cm ⁻¹]	$\nu(\text{C-C})$ (aro.) [cm ⁻¹]	$\nu(\text{C-H})$ [cm ⁻¹]
-OH		1710		
-O ⁻ , Na ⁺		1580		
-(CH ₂) ₁₇ CH ₃	2923, 2849	1663, 1642		1477
-4-NH(C ₆ H ₄)(CH ₂) ₁₃ CH ₃	2922, 2843	1655	1519	1450
-O ⁻ , ⁺ NH ₃ (CH ₂) ₁₇ CH ₃	2920, 2850	1579		1466
-O ⁻ , 4 ⁻ NH ₂ (C ₆ H ₄)(CH ₂) ₁₃ CH ₃	2922, 2849	1598	1519	1452

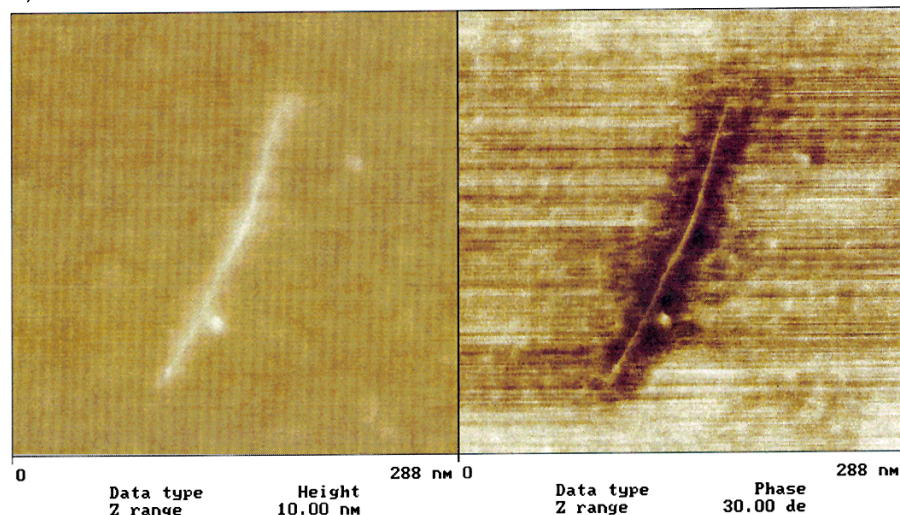
¹H NMR (200 MHz, CD₂Cl₂) of the s-SWNTs shows the presence of the alkyl-aryl amide as the terminating functionality of the SWNTs: δ 0.88 (3H, broad s, CH₃), δ 1.26–1.61 (24H, broad multiplet, 12 × CH₂), δ 2.56 (2H, very broad s, α -CH₂), and δ 7.16 (4H, very broad s, 4 × CH, aromatic). The breadth of the aromatic peak is probably due to the rigid nature of the imide bond and the partial orientation of the magnetically anisotropic SWNT in the magnetic field. This latter effect serves to broaden all of the other resonances in the side chain.

The Raman spectrum of a sample of s-SWNT-CONH-4-C₆H₄(CH₂)₁₃CH₃ (Fig. 3A) was measured in carbon disulfide, with an excitation frequency of 1064 nm, and it showed radial and tangential modes at $\omega_r = 171$ and $\omega_t = 1591$ cm⁻¹, respectively. A Raman spectrum measured in the solid state (Fig. 3B), using the same excitation frequency, showed $\omega_r = 171$ and $\omega_t = 1590$ cm⁻¹. These modes occur at $\omega_r = 170$ and $\omega_t = 1590$ cm⁻¹ in the previously characterized s-SWNT-CONH(CH₂)₁₇CH₃,^[7] and are similar to the Raman spectra of insoluble SWNTs.^[9]

The near-IR spectra of s-SWNTs provide direct information on the band electronic spectra of the s-SWNTs.^[7] The near-IR of s-SWNT-CONH-4-C₆H₄(CH₂)₁₃CH₃ (Fig. 4) showed peaks at 10544, 9694, and 9062 cm⁻¹ (1.29, 1.20, and 1.14 eV) for the band transitions in the metallic nanotubes and a peak at 5421 cm⁻¹ (0.67 eV) for the semiconducting nanotubes. These transitions are similar to those seen previously for s-SWNTs,^[7] and are in the same range as reported for other forms of SWNTs.^[4,10–12] Thus the nature of terminating functionality that is used to allow dissolution, does not affect the electronic structure of the SWNTs.

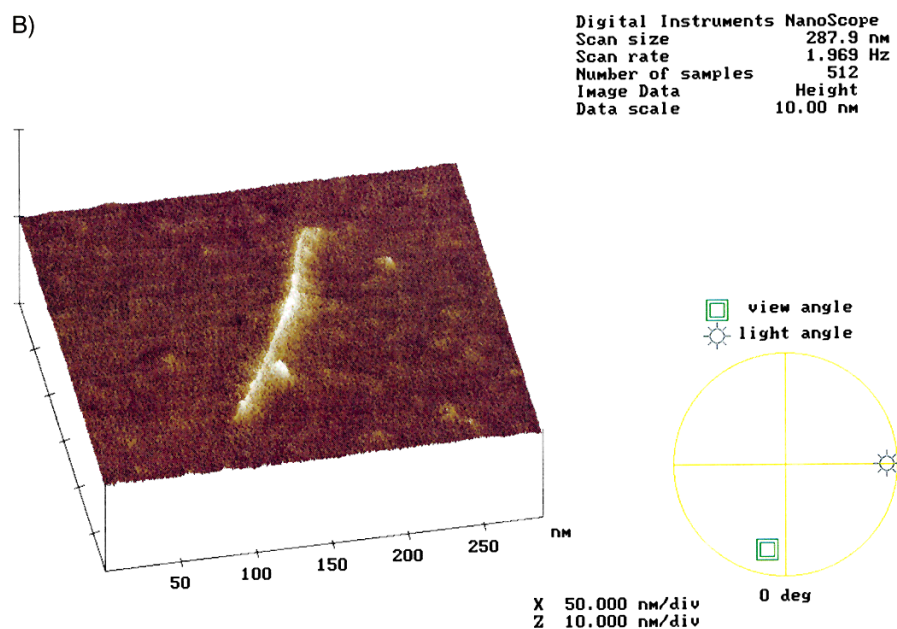
We have recently shown that solution-phase doping of s-SWNTs leads to gross changes in the near-IR spectra of these materials.^[7] These experiments provide direct information on the origin of the changes in conductivity that are observed

A)



nanotub4.003

B)



nanotub4.003

Fig. 1. AFM image of s-SWNT-CONH(CH₂)₁₇CH₃ on mica substrate (Digital Instruments Nanoscope). Measured vertical height of SWNT = 1.2 nm. A) Height and phase scan. B) Angle view.

in solid-phase doping experiments.^[13–16] In the near-IR spectrum of the I₂-doped s-SWNT-CONH-4-C₆H₄(CH₂)₁₃CH₃, the band transition in the semiconducting nanotubes has vanished (Fig. 4), whereas the band transition in the metallic nanotubes is lower in energy, 9601 cm⁻¹ (1.19 eV), than in the pristine s-SWNT, which had band transitions at 10 544, 9694, and 9062 cm⁻¹ (1.31, 1.20, and 1.12 eV). In the case of Br₂ doping the band transition in the metallic nanotubes moved to even lower energy [8590 cm⁻¹ (1.06 eV)] than in the I₂-doped s-SWNT. The absence of the band transition in the acceptor-doped semiconducting nanotubes was previously at-

tributed to the complete depletion of electrons from the first singularity in the density of states (DOS)^[4,12] of the band electronic structure of these SWNTs.^[7] The doping results for s-SWNT-CONH-4-C₆H₄(CH₂)₁₃CH₃ are very similar to those observed for s-SWNT-CONH(CH₂)₁₇CH₃.^[7] Thus we find that the halogen-doping behavior of the s-SWNTs is independent of amide functionality in the case of aryl and alkyl side chains.

The solubility and physical properties of s-SWNTs are similar whether the amide function derives from an alkylamine^[7] or an alkyl-arylamine (this work). We therefore set

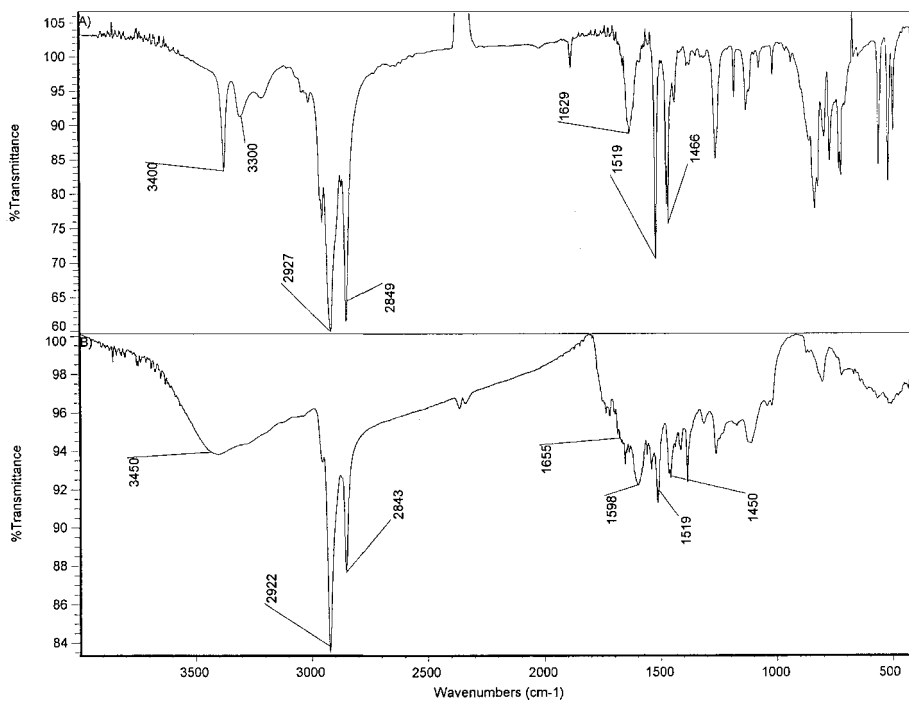
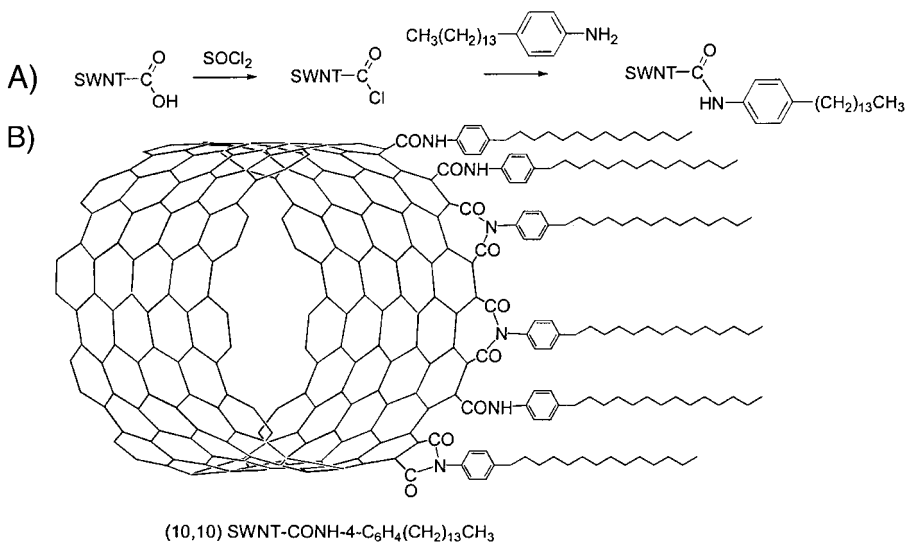


Fig. 2. Mid-IR spectrum of 4-tetradecylamine (KBr pellet, Nicolet Magna-IR 560 E.S.P. spectrometer). A) 4-Tetradecylamine. B) s-SWNT-CONH-4-C₆H₄(CH₂)₁₃CH₃.



Scheme 2. Formation (A) and structure (B) of the SWNT amide.

out to determine the limits of our approach to the production of s-SWNTs.

We began by investigating the susceptibility of unshortened, but purified SWNTs to the end-group derivatization approach. The purified SWNTs are also terminated with carboxylic acid groups, but are much longer, and they are more tenaciously held in bundles. Using the amide functionalization procedure given above, only about 5% of the final product was soluble in CH₂Cl₂. The near-IR spectrum of the soluble portion from this procedure was identical to that of the s-SWNTs obtained from the shortened SWNTs.

The band transitions from the metallic SWNTs had peaks at 10 429, 9691, and 9161 cm⁻¹ (1.29, 1.20, and 1.14 eV) for the shortened, and 10 522, 9701, and 9140 cm⁻¹ (1.30, 1.20, and 1.13 eV) for the unshortened s-SWNTs. The semiconducting bandgaps were at 5421 cm⁻¹ (0.67 eV) for the shortened and at 5400 cm⁻¹ (0.67 eV) for the unshortened s-SWNTs. It is therefore apparent that the soluble fraction from the regular SWNTs is soluble because its length is comparable to that of the shortened s-SWNT or because these tubes are already exfoliated into individual nanotubes and small bundles.

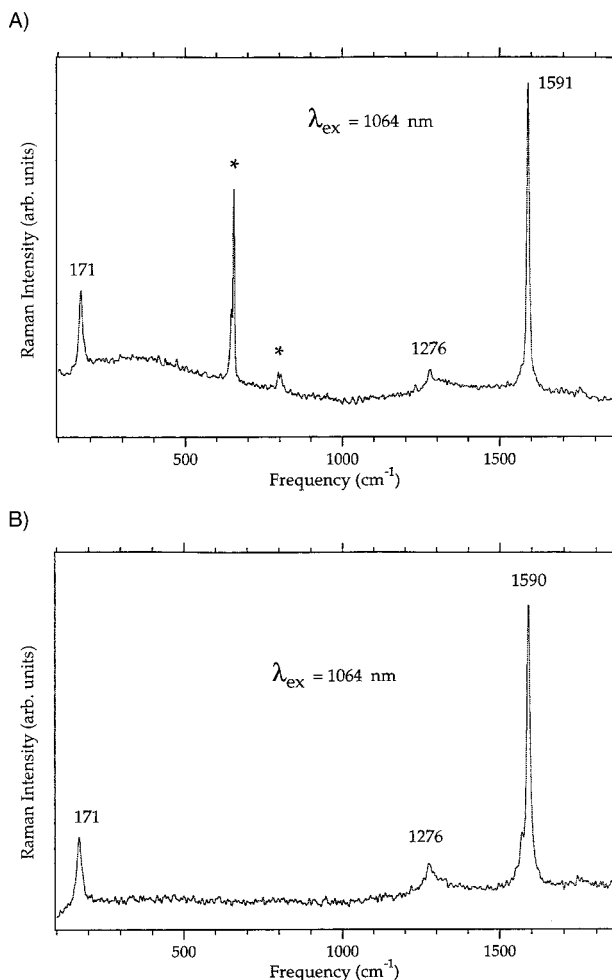
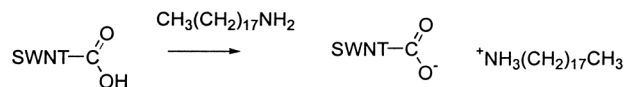


Fig. 3. FT-Raman spectra of s-SWNT-CONH-4-C₆H₄(CH₂)₁₃CH₃ (1064 nm excitation from Nd:YAG, BOMEM DA3 spectrometer): A) In CS₂ solution. The peaks labeled with an asterisk are due to CS₂. B) In the solid state.

After reaction of the amine with the acid chloride form of the shortened SWNT, the product is not entirely soluble. Of the product that is soluble, around 85–90 % is soluble in solvents such as tetrahydrofuran (THF), CH₂Cl₂, and CS₂, while a further 10–15 % is soluble in pyridine. The near-IR spectra of these two solutions are slightly different (Fig. 5). For the semiconducting s-SWNTs: the pyridine-soluble sample shows a lower-energy transition than that of the sample soluble in other solvents (as well as pyridine). It would also appear that the pyridine-soluble s-SWNTs give rise to three distinct peaks in the region of the semiconducting band transitions while normally there is only a single broad peak. The band transitions of the SWNTs soluble in other solvents are at 10494, 9768, and 9133 cm⁻¹ (1.30, 1.21, and 1.12 eV) for the metallic fraction and at 5427 cm⁻¹ (0.67 eV) for the semiconducting component. For the s-SWNTs that are only soluble in pyridine, the corresponding transitions occur at 10651, 9777, and 9105 cm⁻¹ (1.32, 1.21, 1.13 eV) and 5472, 5272, and 5132 cm⁻¹ (0.68, 0.65, 0.64 eV). On the basis of the previous correlation,^[9] it would be expected that this shift in transition energies im-

plies that the pyridine-soluble fraction is of slightly larger diameter than the regular s-SWNT.^[7]

We then attempted the simplest possible route to the dissolution of the SWNTs by directly reacting the amine with the shortened SWNT-COOH (Scheme 3). Thus we ran a simple acid–base reaction in the hope of producing a zwitterion. For this reaction we used octadecylamine.^[7] This method produced SWNTs that were soluble in THF. The near-IR of the s-SWNTs produced in this method are very similar to s-SWNTs that were produced with the covalent functionalization approach.^[7] The near-IR spectrum of these SWNTs (Fig. 6) showed peaks at 10268, 9690, and 9112 cm⁻¹ (1.27, 1.20, and 1.13 eV) for the metallic band transitions, and a peak at 5389 cm⁻¹ (0.67 eV) for the semiconducting band transitions. The amine is associated with the SWNT via an ionic bond and this is reflected in the mid-IR, which shows a peak at 1579 cm⁻¹ due to the carboxylate anion stretch mode. The NMR of this sample is very broad, with peaks at δ 0.87 (CH₃), 1.21 (CH₂), and 3.49 (α-CH₂). The s-SWNT-COO⁻ ·⁺NH₃(CH₂)₁₇CH₃ were found to be soluble in THF and CH₂Cl₂.



Scheme 3. Reaction of the amine CH₃(CH₂)₁₇NH₃ with the shortened SWNT-COOH.

We also attempted to produce soluble SWNTs by formation of the amide from aniline. The use of aniline instead of 4-tetradecylaniline produced SWNTs that were almost completely insoluble in CH₂Cl₂. A very small fraction was soluble in THF and an even larger, although still small, fraction was soluble in aniline. It is therefore likely that a long alkyl chain on the amide functionality is necessary to obtain soluble SWNTs.

In conclusion, we have demonstrated a number of strategies that lead to soluble SWNTs (s-SWNTs). In particular we have shown that it is possible to obtain s-SWNTs by the covalent attachment of long alkyl chains via formation of amides, and by the formation of zwitterions through an acid–base reaction. These techniques will play a vital role in the production of engineered materials based on SWNTs.

Experimental

Preparation of s-SWNT-CONH-4-C₆H₄(CH₂)₁₃CH₃: Shortened SWNTs [5] (2.01 g) in 45 mL of SOCl₂ together with 12 drops of dimethylformamide (DMF), were stirred together at 70 °C for 24 h. The mixture was cooled and centrifuged at 2000 rpm for 30 min. The excess SOCl₂ was decanted and a black solid recovered and dried under vacuum (final weight of SWNT-COCl: 1.821 g).

SWNT-COCl (0.10 g) and 4-tetradecylaniline (0.57 g), were heated at 100 °C for 4 days. During this time the liquid phase became black. After cooling, the solid was repeatedly treated with EtOH and sonicated, and the washings filtered through a membrane (pore size 0.2 μm). The collected solid was washed repeatedly with EtOH to remove free amine. After drying, the black solid was treated with CH₂Cl₂. The black mixture was then filtered through a coarse filter paper and the filtrate taken to dryness on a rotary evaporator (final weight of s-SWNT-CONH-4-C₆H₄(CH₂)₁₃CH₃: 0.06 g).

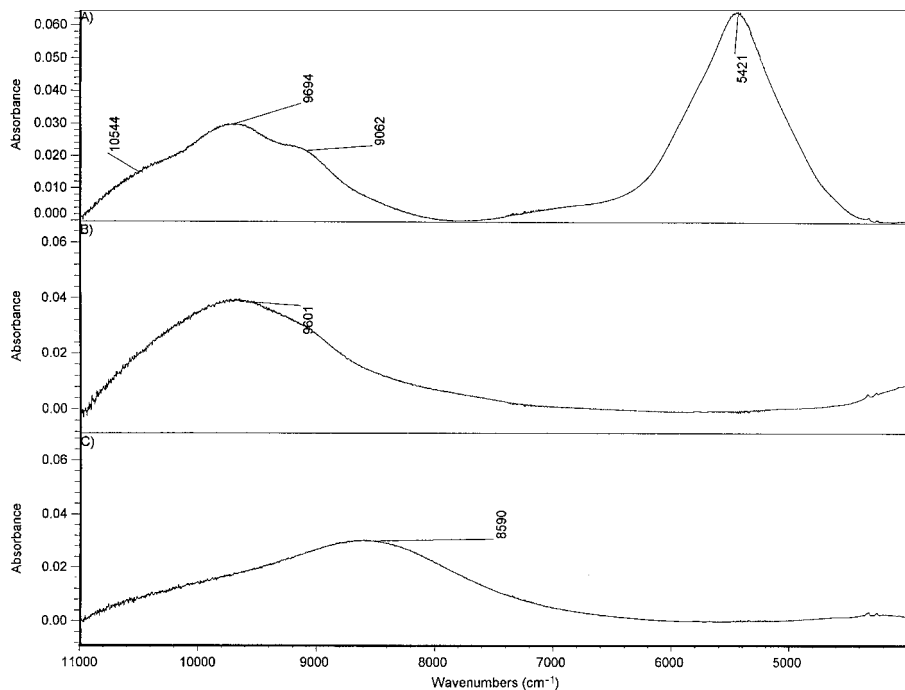


Fig. 4. Near-IR spectrum of s-SWNT-CONH-4-C₆H₄(CH₂)₁₃CH₃ in CS₂ (quartz cell, light path 1 mm, Nicolet Magna-IR 560 E.S.P. spectrometer), at a concentration of 3.3 mg/mL. A) Pristine. B) Saturation doped with I₂. C) Saturation doped with Br₂.

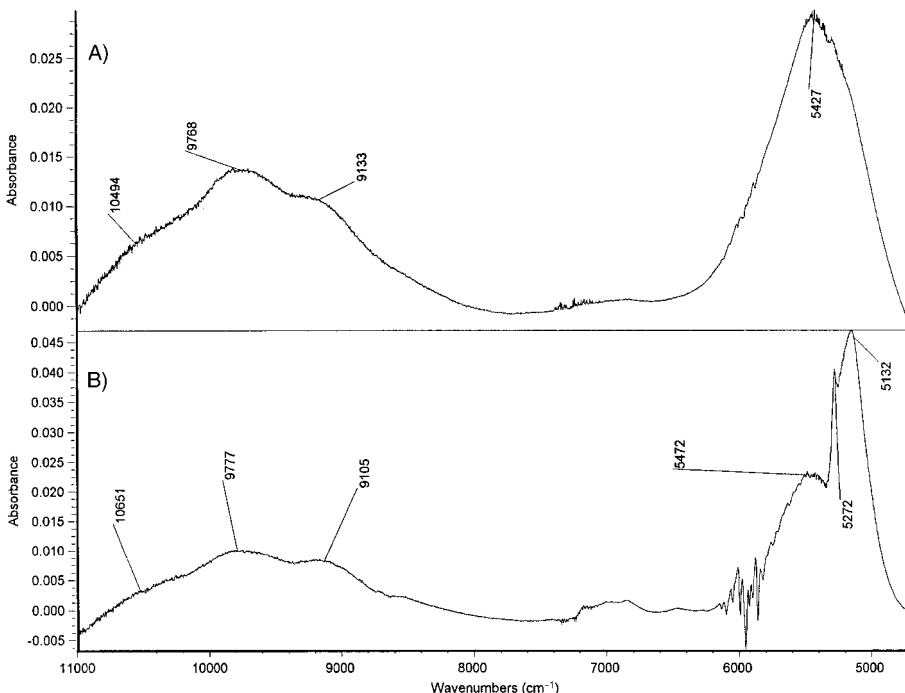


Fig. 5. Near-IR spectrum of s-SWNT-CONH-4-C₆H₄(CH₂)₁₃CH₃ in pyridine (quartz cell, light path 1 mm, Nicolet Magna-IR 560 E.S.P. spectrometer), at a concentration of 1.7 mg/mL. A) Soluble. B) Pyridine-only soluble.

Preparation of s-SWNT-COO⁻ ·NH₃(CH₂)₁₇CH₃: Shortened SWNTs [5] (0.22 g) were heated with octadecylamine (0.50 g) at 90 °C for 96 h. After cooling to room temperature, the black solid was washed with ethanol 5 times and the washings filtered through a membrane (pore-size 0.2 μm), to remove excess amine. The solid was dissolved in THF, filtered through coarse filter paper, and taken to dryness on a rotary evaporator (final weight of s-SWNT-COO⁻ ·NH₃(CH₂)₁₇CH₃: 0.14 g).

Received: October 2, 1998
Final version: March 23, 1999

[1] A. Thess, R. Lee, P. Nikolaev, H. Dai, P. Petit, J. Robert, C. Xu, Y. H. Lee, S. G. Kim, A. G. Rinzler, D. T. Colbert, G. E. Scuseria, D. Tomaneck, J. E. Fischer, R. E. Smalley, *Science* **1996**, 273, 483.

[2] B. I. Yakobson, R. E. Smalley, *Am. Sci.* **1997**, 85, 324.
[3] E. W. Wong, P. E. Sheehan, C. M. Lieber, *Science* **1997**, 277, 1971.
[4] M. S. Dresselhaus, G. Dresselhaus, P. C. Eklund, *Science of Fullerenes and Carbon Nanotubes*, Academic, New York **1996**.
[5] J. Liu, A. G. Rinzler, H. Dai, J. H. Hafner, R. K. Bradley, P. J. Boul, A. Lu, T. Iverson, K. Shelimov, C. B. Huffman, F. Rodriguez-Macias, Y.-S. Shon, T. R. Lee, D. T. Colbert, R. E. Smalley, *Science* **1998**, 280, 1253.
[6] Y. Chen, R. C. Haddon, D. Fang, A. M. Rao, P. C. Eklund, W. H. Lee, E. C. Dickey, E. A. Grulke, J. C. Pendergrass, A. Chavan, B. E. Haley, R. E. Smalley, *J. Mater. Res.* **1998**, 13, 2423.
[7] J. Chen, M. A. Hamon, H. Hu, Y. Chen, A. M. Rao, P. C. Eklund, R. C. Haddon, *Science* **1998**, 282, 95.
[8] Y. Chen, J. Chen, H. Hu, M. A. Hamon, M. E. Itkis, R. C. Haddon, *Chem. Phys. Lett.* **1999**, 299, 532.

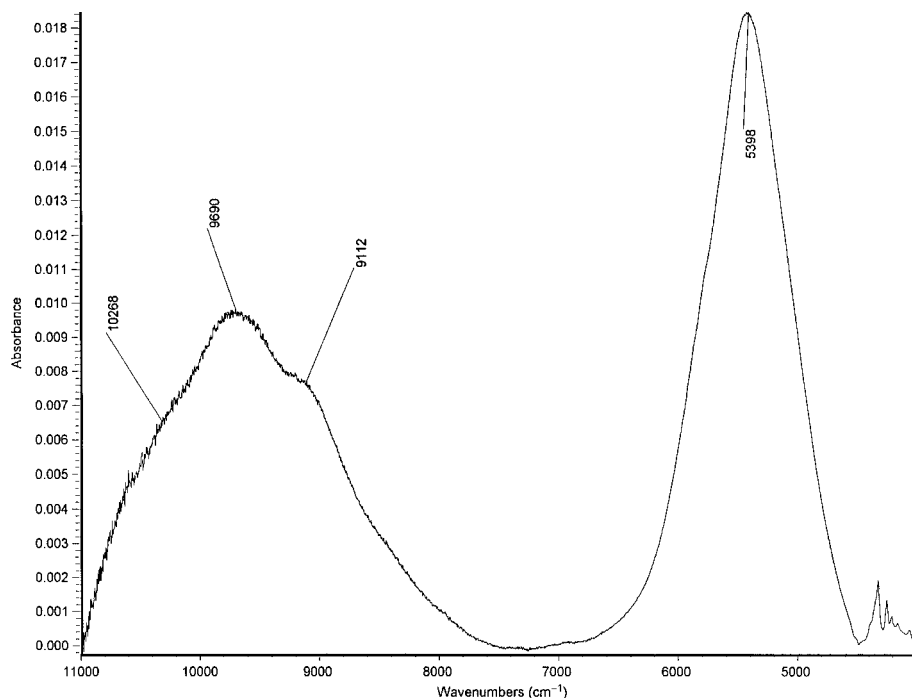


Fig. 6. Near-IR spectrum of s-SWNT-COO⁻, *NH₃(CH₂)₁₇CH₃ (quartz cell, light path 1 mm, Nicolet Magna-IR 560 E.S.P. spectrometer).

- [9] A. M. Rao, E. Richter, S. Bandow, B. Chase, P. C. Eklund, K. A. Williams, S. Fang, K. R. Subbaswamy, M. Menon, A. Thess, R. E. Smalley, G. Dresselhaus, M. S. Dresselhaus *Science* **1997**, *275*, 187.
- [10] J. W. G. Wildoer, L. C. Venema, A. G. Rinzler, R. E. Smalley, C. Dekker, *Nature* **1998**, *391*, 59.
- [11] T. W. Odom, J.-L. Huang, P. Kim, C. H. Lieber, *Nature* **1998**, *391*, 62.
- [12] T. Pichler, M. Knupfer, M. S. Golden, J. Fink, A. Rinzler, R. E. Smalley, *Phys. Rev. Lett.* **1998**, *80*, 4729.
- [13] T. W. Ebbesen, *Phys. Today* **1996**, 26.
- [14] R. S. Lee, H. J. Kim, J. E. Fischer, A. Thess, R. E. Smalley, *Nature* **1997**, *388*, 255.
- [15] A. M. Rao, P. C. Eklund, S. Bandow, A. Thess, R. E. Smalley, *Nature* **1997**, *388*, 257.
- [16] L. Grigorian, K. A. Williams, S. Fang, G. U. Sumanasekera, A. L. Loper, E. C. Dickey, S. J. Pennycook, P. C. Eklund, *Phys. Rev. Lett.* **1998**, *80*, 5560.

Wet-Chemical Synthesis of Doped Colloidal Nanomaterials: Particles and Fibers of LaPO₄:Eu, LaPO₄:Ce, and LaPO₄:Ce,Tb**

By Heike Meyssamy, Karsten Riwotzki, Andreas Kornowski, Sabine Naused, and Markus Haase*

Oxide materials doped with lanthanide ions represent a class of materials with significant technological importance. Bulk crystals of these materials are used, for instance, as la-

ser materials, in lighting applications, and as phosphors in cathode ray tubes.^[1]

Recently, the synthesis and the spectroscopic properties of nanocrystals and nanocrystalline layers of these materials (e.g., lanthanide-doped Y₂O₃^[2-7]) have attracted considerable interest^[8,9] since they are considered as potentially useful active components in new optoelectronic devices.^[10]

Layers of nanocrystalline oxides are frequently prepared by sol-gel methods or vacuum deposition techniques. In contrast, doped nanocrystals of ZnS:Mn,^[11-15] CdS:Mn,^[16-19] and YVO₄:Eu^[20] can be directly crystallized from an aqueous or an organic solution. Since no calcination step is applied, this liquid phase synthesis yields well-separated nanoparticles and even stable colloidal solutions if the synthesis parameters are properly chosen.

As light scattering by separated nanometer-sized particles is negligible, these colloids can be investigated with the same spectroscopic methods as solutions of molecules. For this reason, colloidal solutions of solid nanoparticles have been extensively employed, for instance, by research groups investigating the size-dependent electronic energy structure of II-VI and III-V semiconductor nanocrystals.^[21-27]

In order to prove that the dopant ion is properly incorporated into the crystal lattice, an analytical tool is required that is sensitive to the local environment of the dopant ion in the nanocrystalline host. The standard technique employed is extended X-ray absorption fine structure (EXAFS) spectroscopy, which has been used to probe the dopant site in nanocrystalline Y₂O₃:Tb^[6] and ZnS:Mn.^[13]

A few dopants are known, however, where the luminescence spectrum of the dopant ion itself can be used to probe its crystal environment. The most extensively used

[*] Dr. M. Haase, H. Meyssamy, K. Riwotzki, A. Kornowski, S. Naused Institut für Physikalische Chemie, Universität Hamburg Bundesstrasse 45, D-20146 Hamburg (Germany)

[**] We thank J. Ludwig and Dr. Klaska from the Mineralogisch-Petrographisches Institut of the University of Hamburg for the measurement of the XRD spectra. We gratefully acknowledge funding of this project by the German Science Foundation (DFG).